ChemComm

Cite this: *Chem. Commun.*, 2011, **47**, 11624–11626

www.rsc.org/chemcomm

COMMUNICATION

Au/Pt and Au/Pt_3Ni nanowires as self-supported electrocatalysts with high activity and durability for oxygen reduction†

Yueming Tan,[a] Jingmin Fan,[a] Guangxu Chen,[a] Nanfeng Zheng*[a] and Qingji Xie[b]

Received 8th September 2011, Accepted 22nd September 2011
DOI: 10.1039/c1cc15558j

Novel Au/Pt and Au/Pt_3Ni nanostructures consisting of Pt and Pt_3Ni alloy nanodendrites grown on Au nanowires were synthesized, which exhibited high electrocatalytic activity and durability toward oxygen reduction when used as self-supported catalysts.

Electrochemical energy conversion devices, ranging from fuel cells to metal–air batteries, require effective electrocatalysts for the oxygen reduction reaction (ORR).[1] Currently, most popular ORR electrocatalysts consist of Pt nanoparticles physisorbed on carbon supports of high surface area. However, before such electrocatalysts are ideal for a wide range of practical applications, several critical issues must be addressed. (1) The ORR activity of these Pt nanocatalysts is relatively low owing to the inherently slow oxygen reduction kinetics. (2) Pt surface atoms suffer from serious dissolution and migration during the electrocatalytic process, resulting in aggregation of nanoparticles and deterioration of surface area and catalytic activity.[2] (3) The serious carbon corrosion is also a critical problem with respect to the durability of catalysts.[3]

Recently, Pt-based hetero-nanostructures have shown enhanced electrocatalytic activity.[4] For instance, Pt–Pd bimetallic nanodendrites exhibit much higher ORR activity than commercial Pt catalysts owing to the presence of highly active exposed facets.[4a] Also, the ORR activity of Pt catalysts can be much improved by incorporating other metal(s) to form an alloy with the proper composition and crystal phase.[5] Pt_3Ni is one of the most successful examples for such cases.[5a–e] The high ORR activity of Pt_3Ni is attributed to the weaker OH adsorption arising from the decrease of the d-band center on the Pt skin formed by surface segregation.[5a] However, remarkable improvement has been achieved solely in electrocatalytic activity in most of the above studies. For further evolution of the state-of-the-art Pt-based heterogeneous and alloy nanostructures, synthesis of nanocatalysts with both high activity and excellent durability is highly desirable and technologically important.[6]

One-dimensional (1-D) metal nanostructures have attracted particular attentions due to their excellent electrocatalytic performance.[7] In general, the high conductivity of 1-D metal nanostructures due to the path directing effects of the structural anisotropy is conducive to the reaction kinetics on the catalyst surfaces.[7a–d] Moreover, 1-D metal nanostructures are less vulnerable to dissolution and aggregation than nanoparticles during the electrocatalytic process due to the millimetre-scale length.[7e–h] Despite the fact that 1-D metal nanostructures have high conductivity and structural stability, the development of promising electrocatalysts by utilizing the support effect of 1-D metal nanostructures has not been fully exploited.

Considering that the incorporation of Au can suppress Pt dissolution and migration during ORR,[1c,6b] the growth of Pt or Pt_3Ni alloy on Au nanowires may integrate the advantages of Pt-based bimetallic catalysts with 1-D nanostructures to yield highly active and durable self-supported nanocatalysts. Herein, novel Au/Pt and Au/Pt_3Ni nanowires consisting of Pt and Pt_3Ni alloy nanodendrites grown on Au nanowires were synthesized, which exhibited much enhanced electrocatalytic activity and durability toward ORR when used as self-supported catalysts.

In the first step, we prepared uniform Au nanowires following a reported methodology (Fig. S1, ESI†).[8] These Au nanowires were then used as seeds for the formation of Au/Pt nanowires. The morphologies of the prepared Au/Pt nanowires were examined by scanning electron microscopy (SEM) and transmission electron microscopy (TEM). Typical SEM and TEM images reveal that a dense array of nanodendrites grow on the Au nanowires (Fig. 1a and b and S2a (ESI†)). Fig. 1d shows the high angle annular dark field scanning (HAADF-STEM) image and energy-dispersive X-ray (EDX) elemental mapping of Au and Pt, revealing the heterogeneous structure of the bimetallic nanowires, consisting of Au as the core and a dendritic Pt shell. The heterogeneous structure of the Au/Pt nanowires was also confirmed by X-ray diffraction (XRD). As shown in Fig. S3 (ESI†), obvious Pt peaks can still be distinguished from the strong Au diffraction peaks though they are overlapped to some extent. The HRTEM image (Fig. 1c) indicates that the lattice spacing in the nanodendrites is 0.227 nm, consistent with the (111) lattice spacing of the face centered cubic (fcc) Pt.

[a] *State Key Laboratory for Physical Chemistry of Solid Surfaces and Department of Chemistry, College of Chemistry and Chemical Engineering, Xiamen University, Xiamen 361005, China. E-mail: nfzheng@xmu.edu.cn; Fax: +86 592 2183047; Tel: +86 592 2186821*
[b] *Key Laboratory of Chemical Biology and Traditional Chinese Medicine Research (Ministry of Education of China), College of Chemistry and Chemical Engineering, Hunan Normal University, Changsha 410081, China*

† Electronic supplementary information (ESI) available: Experimental details and data. See DOI: 10.1039/c1cc15558j

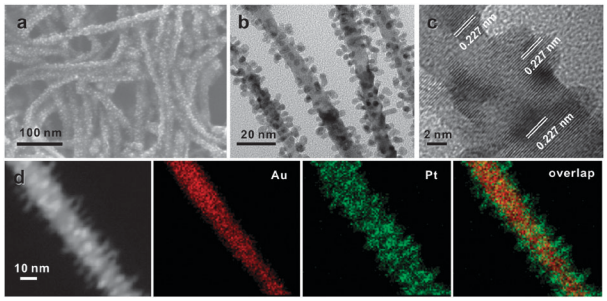

Fig. 1 SEM (a), TEM (b), HRTEM (c) and HAADF-STEM-EDX mapping (d) images of Au/Pt nanowires.

The synthesis of Au/Pt_3Ni nanowires was similar to that of Au/Pt except that an appropriate amount of Ni was introduced, and similar morphologies as Au/Pt nanowires can be observed (Fig. 2a and b and S2b (ESI†)). The structure and composition of Au/Pt_3Ni nanowires were further characterized as follows: (1) The inductively coupled plasma-atomic emission spectroscopy (ICP-AES) result suggests that the molar ratio between Pt and Ni is 2.9 : 1, which is close to 3 : 1. (2) The *d* lattice spacing of the dendritic shell shown in the HRTEM image is 0.222 nm (Fig. 2c), closely matching that of the (111) plane of Pt_3Ni alloy (0.221 nm). (3) As shown in the elemental mapping (Fig. 2d), both Pt and Ni are distributed evenly in the nanodendrites. (4) The diffraction peaks slightly shift to higher angles compared with those for pure Pt (Fig. S3, ESI†). These results clearly indicate the formation of Pt_3Ni alloy nanodendrites on Au nanowires.

The UV-Vis-IR spectra of Au/Pt and Au/Pt_3Ni nanowires display that the surface plasmon peak at 525 nm and the broad band above 900 nm of the Au nanowires are completely damped out by the deposition of Pt or Pt_3Ni (Fig. S4, ESI†). This result suggests that Au nanowires are fully covered by Pt or Pt_3Ni. No obvious Au features are detected in the cyclic voltammograms for Au/Pt and Au/Pt_3Ni nanowires with the upper potential opened to 1.8 V, also confirming little exposed Au atoms on the surface of nanowires (Fig. S5, ESI†). The presence of a Pt-rich outermost layer for Au/Pt_3Ni nanowires is further confirmed by using surface sensitive carbon monoxide (CO) electro-oxidation (Fig. S6, ESI†). The Pt-rich surface should be conducive to preventing Ni from leaching when the Au/Pt_3Ni nanowires are exposed to the hostile electrochemical environments. The ICP-AES results suggest that the molar ratios of Au to Pt are 49 : 51 and 52 : 48 for Au/Pt and Au/Pt_3Ni nanowires, respectively, which are close to the molar ratio of Au nanowires to Pt precursor (1 : 1). The density of dendrites on Au nanowires can be controlled *via* simply changing the molar ratio of Au nanowires to Pt precursor. As shown in Fig. S7 (ESI†), Au/Pt and Au/Pt_3Ni nanowires with fewer dendrites were obtained when the molar ratio of Au nanowires to Pt precursor decreased from 1 : 1 to 2 : 1.

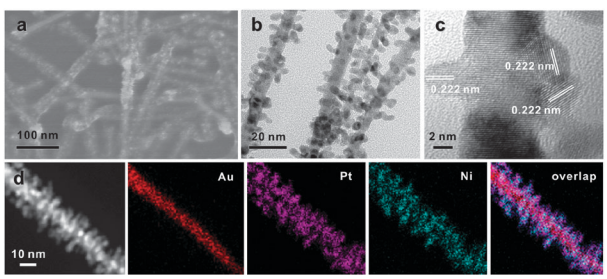

Fig. 2 SEM (a), TEM (b), HRTEM (c) and HAADF-STEM-EDX mapping (d) images of Au/Pt_3Ni nanowires.

After surface treatment with *n*-butylamine by using a reported method,[5d] the Au/Pt and Au/Pt_3Ni nanowires were tested as self-supported nanocatalysts for studying their electrocatalytic activity. The specific electrochemically active surface areas (SEASAs) of Au/Pt and Au/Pt_3Ni catalysts were detected by measuring the areas under the hydrogen adsorption/desorption peaks of the cyclic voltammograms in 0.1 M $HClO_4$ solution (Fig. 3a), assuming that a monolayer of H adatoms requires 210 mC cm^{-2}. The SEASAs of Au/Pt and Au/Pt_3Ni catalysts are 72.3 and 74.2 m^2 g^{-1}, which are a little higher than that of commercial Pt/C catalyst (68.4 m^2 g^{-1}). The high SEASAs of Au/Pt and Au/Pt_3Ni catalysts should be attributed to the small size of the nanodendrites (mostly <3 nm). Although these nanowires were directly used as electrocatalysts without additional carbon supports, they still exhibited extremely large SEASAs, highlighting their high conductivity.

The ORR measurements were performed in O_2-saturated 0.1 M $HClO_4$ solutions at room temperature by using a rotating disk electrode (RDE). A characteristic set of polarization curves for the ORR on Au/Pt_3Ni, Au/Pt and Pt/C catalyst modified RDEs are displayed in Fig. 3b. Two distinguishable potential regions are clearly observed in the polarization curves: the well-defined diffusion limiting current region below 0.6 V and the mixed kinetic-diffusion control region between 0.7 and 1.0 V. The RDE polarization curves show that both Au/Pt_3Ni and Au/Pt catalysts have more positive onset potentials than the Pt/C catalyst. The half-wave potentials ($E_{1/2}$) of Au/Pt_3Ni, Au/Pt and Pt/C are 0.892, 0.870 and 0.849 V, respectively.

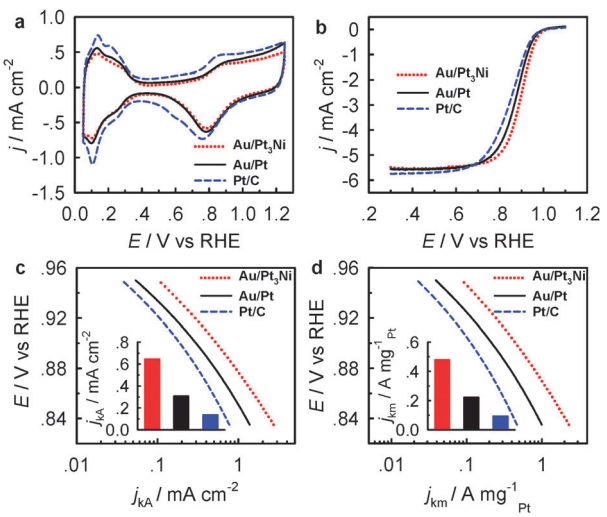

Fig. 3 (a) Cyclic voltammograms for Au/Pt_3Ni, Au/Pt, and Pt/C catalysts at 50 mV s^{-1}. (b) ORR polarization curves for Au/Pt_3Ni, Au/Pt and Pt/C catalysts recorded at room temperature in an O_2-saturated 0.1 M $HClO_4$ aqueous solution with a sweep rate of 10 mV s^{-1} and a rotation rate of 1600 rpm. (c, d) Specific activity (j_{kA}) and mass activity (j_{km}) for these three catalysts, which are given as kinetic current densities (j_k) normalized to the real Pt surface areas and the Pt mass, respectively. Insets show the activities at 0.9 V.

In order to compare the activity of different catalysts, the kinetic currents in the kinetic-diffusion control regions, which are normalized to both the real Pt surface areas and the Pt mass, are calculated from the ORR polarization curves by using mass-transport correction (Fig. 3c and d). The Au/Pt catalyst exhibits a specific activity (j_{kA}) of 0.308 mA cm^{-2} at 0.9 V, which is 2.3 times that of Pt/C (0.136 mA cm^{-2}). The specific activity of Au/Pt nanowires is also much higher than that of Au/Pt core/shell nanoparticles reported previously ($\sim$0.2 mA cm^{-2} at 0.8 V),[4c] which may highlight the superior support effect of 1-D nanostructures. The corresponding mass activity (j_{km}) of the Au/Pt catalyst is 0.223 mA μg^{-1}_{Pt}, which is 2.4 times that of Pt/C (0.093 mA μg^{-1}_{Pt}). The high mass activity of the Au/Pt catalyst can be explained as follows: (1) The Au/Pt catalyst provides high SEASA due intrinsically to the dendritic morphology. (2) The Au/Pt catalyst offers facile pathways for electron transfer owing to the incorporation of ultralong 1-D Au nanowires. (3) The nanodendrites on Au nanowires tend to possess (111)-orientation-rich Pt surfaces that possess high activity toward ORR (Fig. S8, ESI†). As expected, the Au/Pt_3Ni catalyst exhibits a further enhanced ORR activity owing to the alloy effect of Pt and Ni. For instance, the specific activity at 0.9 V is 0.646 mA cm^{-2}, which is much higher than those of Pt/C and Au/Pt catalysts. The corresponding mass activity is 0.479 mA μg^{-1}_{Pt}, 5.2 and 2.1 times those of Pt/C and Au/Pt catalysts. The mass activity of Au/Pt_3Ni nanowires is almost higher than that of recent Pd–Pt bimetallic nanodendrites (0.241 ± 0.013 mA μg^{-1}_{Pt})[4a] and carbon black-supported Pt_3Ni nanoctahedra ($\sim$0.3 mA μg^{-1}_{Pt}).[5c]

The electrochemical stability of the catalysts was also investigated by the accelerated durability tests, which were carried out at room temperature in O_2-saturated 0.1 M $HClO_4$ solutions by applying cyclic potential sweeps between 0.6 and 1.1 V at 50 mV s^{-1}. As shown in Fig. S9 (ESI†), the Au/Pt, Au/Pt_3Ni and Pt/C catalysts showed losses of 6.8%, 9.9% and 37.9% in SEASA after 5000 potential cycles, respectively. As a result, the Au/Pt, Au/Pt_3Ni and Pt/C catalysts retained 89.7%, 86.4% and 53.2% of initial mass activities at 0.9 V, respectively. The morphologies of these electrocatalysts after durability tests were characterized by TEM, as shown in Fig. S10 (ESI†). Although serious sintering and aggregation were observed for the Pt/C catalyst, the morphologies of the self-supported Au/Pt and Au/Pt_3Ni catalysts were still maintained, highlighting the excellent structural stability of these nanowires. The enhanced durability can be explained as follows: (1) The presence of subsurface Au atoms can make a remarkable contribution to the durability enhancement of the Pt skin layer based on the well-known place-exchange mechanism.[6b] (2) Compared with the weak interactions between carbon supports and Pt nanoparticles, the stronger interactions between Pt or Pt_3Ni dendritic shell and Au core should be conducive to the durability enhancement. (3) Au is stable in the given potential range for ORR, which can avoid structural instability arising from the support corrosion at high potentials.

In summary, we have successfully synthesized Au/Pt and Au/Pt_3Ni nanowires consisting of small-sized Pt and Pt_3Ni nanodendrites on Au nanowires. The Au/Pt and Au/Pt_3Ni nanowires can be used as self-supported electrocatalysts to offer enhanced electrocatalytic activity and durability toward ORR. The strategy reported here may be helpful for further evolution of the recent state-of-the-art Pt-based heterogeneous and alloy nanostructures.

This work is supported by NSFC (21131005, 21021061, 20925103, 20871100), the MOST of China (2011CB932403, 2009CB930703), the NSF of Fujian Province (Distinguished Young Investigator Grant 2009J06005), the Fok Ying Tung Education Foundation (121011), and the Key Scientific Project of Fujian Province (2009HZ0002-1). Y. M. Tan also acknowledges the support of China Postdoctoral Science Foundation (20100480716).

Notes and references

1 (*a*) B. C. H. Steele and A. Heinzel, *Nature*, 2001, **414**, 345; (*b*) H. A. Gasteiger and N. M. Markovic, *Science*, 2009, **324**, 48; (*c*) J. Zhang, K. Sasaki, E. Sutter and R. R. Adzic, *Science*, 2007, **315**, 220.
2 P. J. Ferreira, G. J. la O', Y. Shao-Horn, D. Morgan, R. Makharia, S. Kocha and H. A. Gasteiger, *J. Electrochem. Soc.*, 2005, **152**, A2256.
3 V. T. T. Ho, C. J. Pan, J. Rick, W. N. Su and B. J. Hwang, *J. Am. Chem. Soc.*, 2011, **133**, 11716.
4 (*a*) B. Lim, M. Jiang, P. H. Camargo, E. C. Cho, J. Tao, X. Lu, Y. Zhu and Y. Xia, *Science*, 2009, **324**, 1302; (*b*) Z. Peng and H. Yang, *J. Am. Chem. Soc.*, 2009, **131**, 7542; (*c*) Y. Kim, J. W. Hong, Y. W. Lee, M. Kim, D. Kim, W. S. Yun and S. W. Han, *Angew. Chem., Int. Ed.*, 2010, **49**, 10197; (*d*) K. M. Yeo, S. Choi, R. M. Anisur, J. Kim and I. S. Lee, *Angew. Chem., Int. Ed.*, 2011, **50**, 745; (*e*) J. Wu, Y. Hou and S. Gao, *Nano Res.*, 2011, **4**, 836.
5 (*a*) V. R. Stamenkovic, B. Fowler, B. S. Mun, G. Wang, P. N. Ross, C. A. Lucas and N. M. Markovic, *Science*, 2007, **315**, 493; (*b*) J. Snyder, T. Fujita, M. W. Chen and J. Erlebacher, *Nat. Mater.*, 2010, **9**, 904; (*c*) J. Zhang, H. Yang, J. Fang and S. Zou, *Nano Lett.*, 2010, **10**, 638; (*d*) J. Wu, J. Zhang, Z. Peng, S. Yang, F. T. Wagner and H. Yang, *J. Am. Chem. Soc.*, 2010, **132**, 4984; (*e*) J. Wu, A. Gross and H. Yang, *Nano Lett.*, 2011, **11**, 798; (*f*) V. R. Stamenkovic, B. S. Mun, M. Arenz, K. J. J. Mayrhofer, C. A. Lucas, G. Wang, P. N. Ross and N. M. Markovic, *Nat. Mater.*, 2007, **6**, 241; (*g*) S. Mukerjee, S. Srinivasan and M. P. Soriaga, *J. Electrochem. Soc.*, 1995, **142**, 1409; (*h*) M. Watanabe, K. Tsurumi, T. Mizukami, T. Nakamura and P. Stonehart, *J. Electrochem. Soc.*, 1994, **141**, 2659; (*i*) S. Koh, J. Leisch, M. F. Toney and P. Strasser, *J. Phys. Chem. C*, 2007, **111**, 3744.
6 (*a*) V. Mazumder, M. Chi, K. L. More and S. Sun, *J. Am. Chem. Soc.*, 2010, **132**, 7848; (*b*) C. Wang, D. v. d. Vliet, K. L. More, N. J. Zaluzec, S. Peng, S. Sun, H. Daimon, G. Wang, J. Greeley, J. Pearson, A. P. Paulikas, G. Karapetrov, D. Strmcnik, N. M. Markovic and V. R. Stamenkovic, *Nano Lett.*, 2011, **11**, 919.
7 (*a*) C. X. Xu, L. Q. Wang, R. Y. Wang, K. Wang, Y. Zhang, F. Tian and Y. Ding, *Adv. Mater.*, 2009, **21**, 2165; (*b*) J. Snyder, P. Asanithi, A. B. Dalton and J. Erlebacher, *Adv. Mater.*, 2008, **20**, 4883; (*c*) L. Liu, E. Pippel, R. Scholz and U. Gösele, *Nano Lett.*, 2009, **9**, 4352; (*d*) S. Guo, S. Dong and E. Wang, *Chem. Commun.*, 2010, **46**, 1869; (*e*) Z. Chen, M. Waje, W. Li and Y. Yan, *Angew. Chem., Int. Ed.*, 2007, **46**, 4060; (*f*) C. Xu, H. Wang, P. K. Shen and S. P. Jiang, *Adv. Mater.*, 2007, **19**, 4256; (*g*) S. J. Guo, S. J. Dong and E. K. Wang, *Energy Environ. Sci.*, 2010, **3**, 1307; (*h*) C. Koenigsmann and S. S. Wong, *Energy Environ. Sci.*, 2011, **4**, 1161; (*i*) C. H. Cui, H. H. Li and S. H. Yu, *Chem. Sci.*, 2011, **2**, 1611; (*j*) C. Koenigsmann, W. P. Zhou, R. R. Adzic, E. Sutter and S. S. Wong, *Nano Lett.*, 2010, **10**, 2806; (*k*) S. Sun, F. Jaouen and J. P. Dodelet, *Adv. Mater.*, 2008, **20**, 3900.
8 C. Wang, Y. Hu, C. M. Lieber and S. Sun, *J. Am. Chem. Soc.*, 2008, **130**, 8902.

